[22] *P. M. Wood*, FEBS Letters *44*, 22 (1974).
[23] *P. George*, J. chem. Soc. *1954*, 4349.
[24] See e.g. *S. Fallab*, Angew. Chem. internat. Ed. *6*, 496 (1967); *R. C. Wilkins* in 'Bioinorganic Chemistry', Adv. chem. Ser. 100, R. F. Gould, Ed., Amer. chem. Soc. Publ., Washington 1971, p. 111.
[25] *T. A. Kaden & S. Fallab* in 'Advances in the Chemistry of the Coordination Compounds', S. Kirschner, Ed., Macmillan Comp., New York 1961, p. 654.
[26] *F. Haber & J. Weiss*, Proc. Roy. Soc. Ser. A *147*, 332 (1934).
[27] *V. M. Berdnikov, Y. N. Kozlov & A. P. Purmal*, Chim. Vys. Energ. *3*, 370 (1969).
[28] *Y. N. Kozlov & V. M. Berdnikov*, Z. Fiz. Chim. *47*, 598 (1973).
[29] *H. J. Forman & I. Fridovich*, Arch. Biochemistry Biophysics *158*, 396 (1973).

155. The Electronic Structure of Azuleno[1,2,3-*cd*]phenalene and Azuleno[5,6,7-*cd*]phenalene, a Comparison

by **Rolf Gleiter**[1], **Jens Spanget-Larsen**[1], **Erik W. Thulstrup**[1,2], **Ichiro Murata**[3], **Kazuhiro Nakasuji**[3] and **Christian Jutz**[4]

Institut für Organische Chemie der Technischen Hochschule D-61 Darmstadt (West-Germany); Department of Chemistry, Faculty of Science, Osaka University, Toyonaka, Osaka 560 (Japan); Organisch Chemisches Institut der Technischen Universität D-8 München (West-Germany).

(18. III. 76)

Summary. The photoelectron (PE.) spectra of azuleno[1,2,3-*cd*]phenalene (**1**) and azuleno[5,6,7-*cd*]phenalene (**2**) have been recorded. The first five bands of both compounds could be assigned to transitions corresponding to removal of electrons from $4a_2$, $6b_1$, $5b_1$, $3a_2$ and $4b_1$ orbitals. This assignment is based mainly on a comparison between the observed ionization potentials and orbital energies calculated in a HMO and a PPP model.

The UV./VIS. polarized absorption spectrum of **1** in the region 10000–45000 cm^{-1} has been measured by means of the stretched film technique. The measurements were performed in polyethylene sheets at 77 °K. Several bands could be assigned to $\pi^* \leftarrow \pi$ transitions calculated by a PPP-CI method.

A comparison between the electronic structures of **1** and **2** is made by means of a simple HMO diagram.

Azuleno[1,2,3-*cd*]phenalene (**1**) and azuleno[5,6,7-*cd*]phenalene (**2**) offer interesting opportunities for the application of perturbation theoretical arguments [1] in deriving their electronic structures from fragments. Two possibilities for **1** and **2**

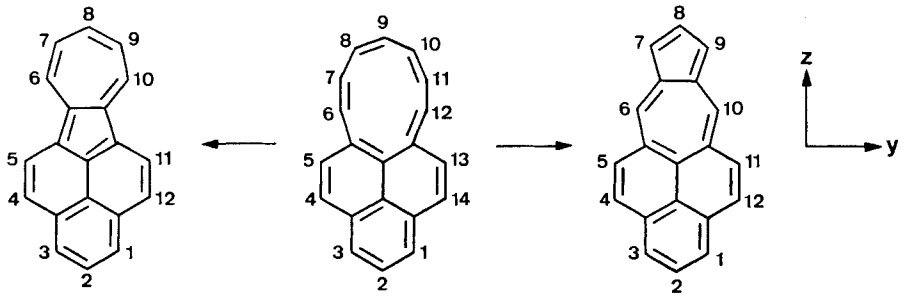

1 **3** **2**

[1] Darmstadt.
[2] Permanent address: Department of Chemistry, Aarhus University, DK-8 Aarhus, Denmark.
[3] Osaka.
[4] München.

are suggestive as shown below: Either one formally adds *m*-divinylbenzene to azulene in such a manner that C_{2v} symmetry is preserved or one introduces an additional bond in 10-annuleno[*cd*]phenalene (**3**) between positions 6 and 12 or 7 and 11 to yield **1** or **2**.

The recent synthesis of **1** [2] and **2** [3] permits a comparison of the electronic structures of the two compounds. The UV./VIS. polarized absorption spectrum and the MCD. spectrum of **2** have been published by *Thulstrup et al.* [5]. In this paper we will report the photoelectron (PE.) spectra of **1** and **2** and the polarized electronic absorption spectrum of **1** in stretched polyethylene film, using the procedure of *Eggers et al.* [4].

PE. Spectra. – For the interpretation of the PE. spectra *Koopmans'* theorem [7] is used. In this approximation the orbital energy ε_J is set equal to minus the measured vertical ionization potential $I_{V,J}$:

$$\varepsilon_J = -I_{V,J}$$

The PE. spectra of **1** and **2** between 6 eV and 12 eV are shown in Fig. 1. The spectra show remarkable differences in the region between 6 eV and 10 eV.

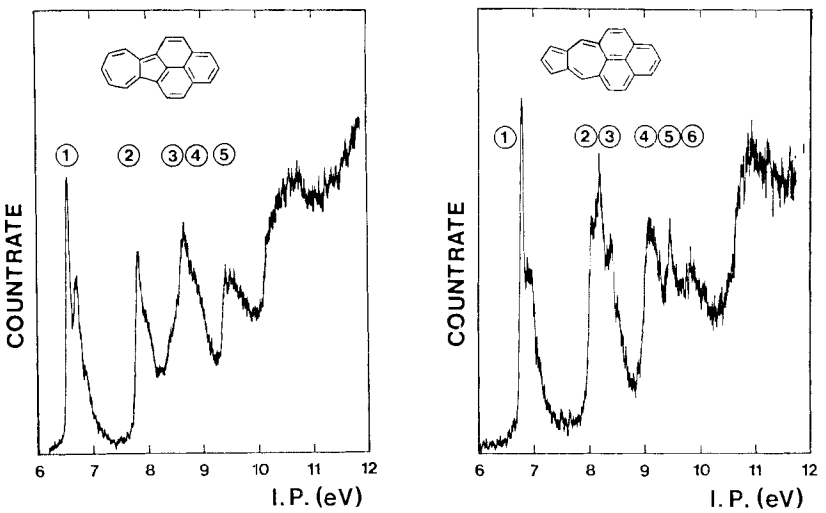

Fig. 1. *Photoelectron spectra of azuleno[1,2,3-*cd*]phenalene* (**1**) *and azuleno[5,6,7-*cd*]phenalene* (**2**)

If it is assumed that the first peak in both spectra is due to a single transition (the transition from the ground state of **1** or **2** to the ground state of the corresponding molecular ion) then the half-height-width of the third peak in the PE. spectrum of **1** and that of the second peak in the PE. spectrum of **2** indicate that each of these peaks are due to two transitions. This is supported by the calculated results listed in Table 1. Here measured ionization potentials are compared with ionization energies calculated by the method of *Brogli* & *Heilbronner* [8] and ionization potentials calculated in the PPP model [9] according to:

$$I^{PPP}_{V,J} = -0.9\,\varepsilon_J - 0.6$$

This formula was derived [10] by comparison of MO calculations with PE. spectra of a large number of planar cyclic conjugated hydrocarbons.

Table 1. *Vertical ionization potentials* $I_{V,J}$ *and* Koopmans' *values* $(-\varepsilon_J)$ *of* **1** *and* **2**. All values in eV.

Experiment				Calculation	
Compound	band	$I_{V,J}$	Assignment	HMO [8]	PPP [9, 10]
	①	6.58	$4a_2$	6.67 ($4a_2$)	6.52 ($4a_2$)
	②	7.85	$6b_1$	8.15 ($6b_1$)	8.10 ($6b_1$)
1	③	8.6	$5b_1$	8.89 ($5b_1$)	8.66 ($5b_1$)
	④	8.9	$3a_2$	9.22 ($3a_2$)	8.72 ($3a_2$)
	⑤	9.43	$4b_1$ or σ	9.82 ($4b_1$)	9.54 ($4b_1$)
	①	7.76	$4a_2$	7.01 ($4a_2$)	6.89 ($4a_2$)
	②	8.05	$6b_1$	8.28 ($6b_1$)	8.22 ($6b_1$)
2	③	8.25	$3a_2$	8.51 ($3a_2$)	8.45 ($3a_2$)
	④	9.05	$5b_1$	9.27 ($5b_1$)	9.21 ($5b_1$)
	⑤	9.43	$4b_1$ or σ	9.50 ($4b_1$)	9.37 ($4b_1$)
	⑥	9.79	$2a_2$ or σ	10.00 ($2a_2$)	10.07 ($2a_2$)

A further confirmation of the assignment given in Table 1 is found in the steep ascent of the first peaks which we attribute to ionization from π orbitals.

The strong overlap of bands ③ and ④ in the PE. spectrum of **1** can be explained by the result that the π MO's $3a_2$ and $5b_1$ are degenerate within the HMO model (see Fig. 4).

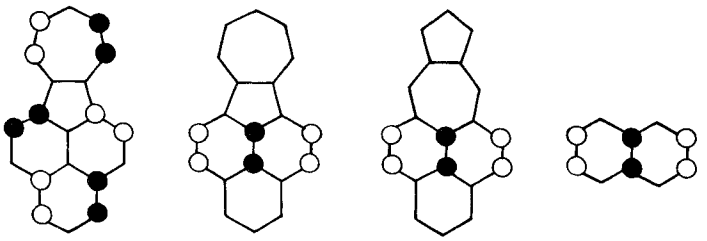

The $3a_2$ and $5b_1$ orbitals of **1** and the $5b_1$ orbital of **2** are composed of localized ethylene fragments as shown above. An orbital with a shape equivalent to $3a_2$ of **1** is not possible in **2** for topological reasons.

In the simple HMO model the $5b_1$ orbitals of **1** and **2** are degenerate with the $2b_{1u}$ orbital of naphthalene (see above) with orbital energy $\varepsilon = \alpha + 1\beta$. A PPP calculation does not delocalize these orbitals to any significant extent (1–2%). Nevertheless, as a result of the SCF procedure, the $5b_1$ orbital of **2** is stabilized and the $5b_1$ orbital of **1** is destabilized with respect to the $2b_{1u}$ orbital of naphthalene. (With the PPP method we obtain: **1** ($5b_1$): -10.29 eV, **2** ($5b_1$): -10.90 eV and naphthalene ($2b_{1u}$): -10.48 eV.) This is due to the fact that both compounds **1** and **2** are non-alternant hydrocarbons. Due to the electronegative character of the five-membered ring and the electropositive character of the seven-membered ring different potentials are obtained in the regions of the highly localized $5b_1$ orbitals of the two compounds. This is visualized in Fig. 2, where the relative atomic potentials are represented graphically. The lengths of the bars in the diagram correspond to the quantities $\Delta F_{\mu\mu} = F^{SCF}_{\mu\mu} - F^{O}_{\mu\mu}$ where $F^{O}_{\mu\mu}$ and $F^{SCF}_{\mu\mu}$ are diagonal elements of the PPP *Fock*-matrix before and after the SCF procedure, respectively. Note that

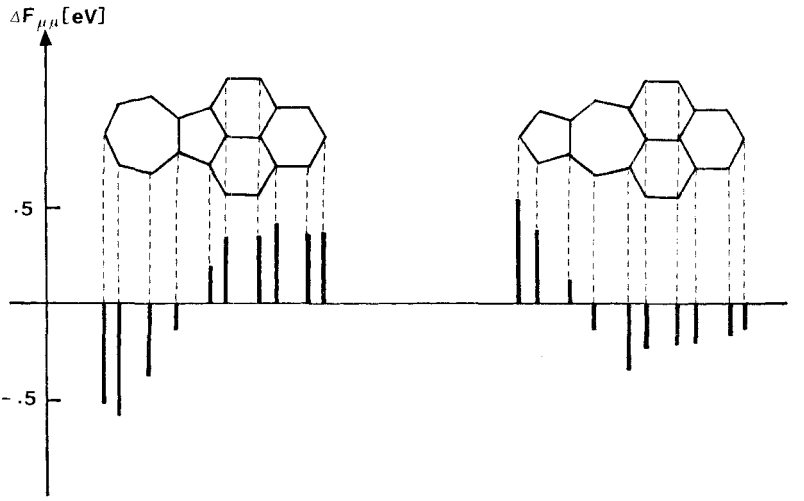

Fig. 2. *Relative self-consistent PPP potentials at the carbon positions in* **1** *and* **2** (see the text)

electron density in a region where ΔF is positive leads to a destabilization and *vice versa*.

During the SCF process, the potentials in the nonalternant hydrocarbons **1** and **2** are changed in different manners. For **1** (Fig. 2a) the potential in the five- and six-membered rings is increased compared to that of an alternant hydrocarbon, which leads to a destabilization of the $5b_1$ orbital of **1**. For **2** (Fig. 2b), however, the potential in the region of the six-membered rings is reduced. This yields a stabilization of the $5b_1$ orbital of **2** with respect to the $2b_{2u}$ orbital of naphthalene.

As a corollary of the theoretical discussion we expect that the ionization potential corresponding to the $2b_{1u}$ orbital of naphthalene lies between the ionization potentials of the $5b_1$ orbitals of **1** and **2**. According to the assignment, given in Table 1, the observed ionization potential for $2b_{1u}$ of naphthalene (8.88 eV) [11] is intermediate between $5b_1$ of **1** (8.66 eV) and $5b_1$ of **2** (9.21 eV). This lends further support to our interpretation of these bands.

In the comparison of the PE. spectra of **1** and **2** (Fig. 3), the most remarkable feature is the much larger energy difference found in **1** between the peaks corre-

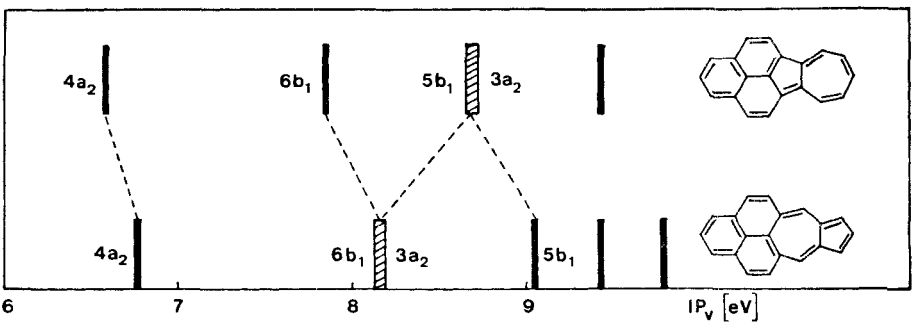

Fig. 3. *Correlation of the first bands in the PE. spectra of* **1** *and* **2**

sponding to the $4a_2$ and $3a_2$ orbitals. This can be understood by simple first order perturbation arguments applied to 10-annuleno[*cd*]phenalene (**3**). The MO correlation diagram (Fig. 4) of **1**, **2** and **3** shows clearly that introduction of a bond in **3** between atoms 7 and 11 will increase the energy of orbital $2a_2$ considerably, whereas introduction of a bond between atoms 6 and 12 will raise the energy of $4a_2$ the most. This means that the energy splitting between the $3a_2$ and $4a_2$ orbitals will be much larger

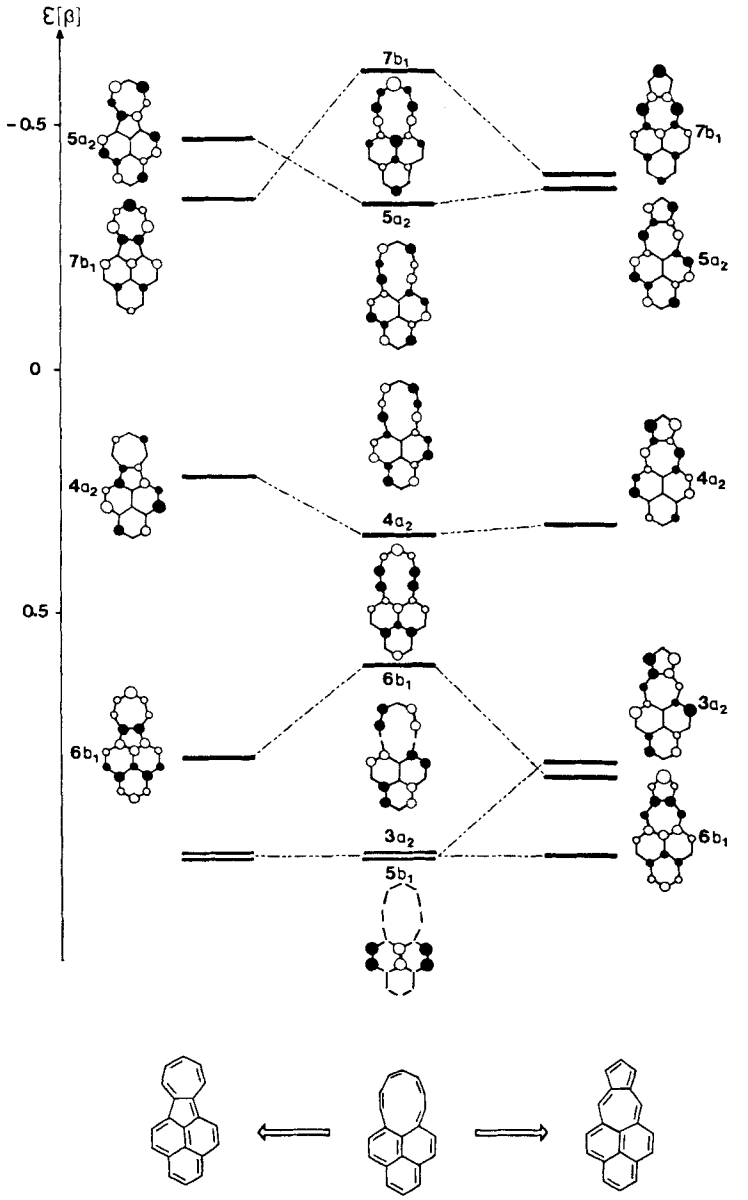

Fig. 4. *Intramolecular HMO interaction diagram of 10-annuleno* [cd]*phenalene to yield* **1** *and* **2**

in **1** than in **2**. It can be mentioned that the lowest unoccupied orbital of **3**, $5a_2$, is shifted similarly to $4a_2$ when going to **1** and **2**. This is one of the reasons for the small energy difference between $7b_1$ and $5a_2$ in **2**, as discussed elsewhere [5] [12].

Electronic absorption spectra of 1 and 2. – The low temperature absorption spectrum of **1** in stretched polyethylene film is given in Fig. 5. The curves were

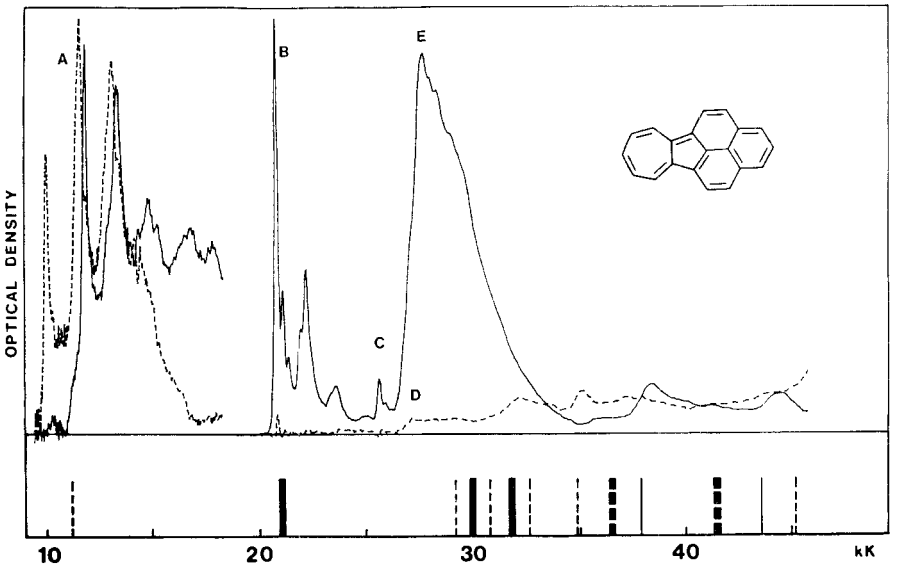

Fig. 5. *Top: Polarized electronic absorption spectrum of* **1** *in stretched polyethylene sheets at 77°K.* The full line represents the long axis polarized and the dashed line the short axis polarized reduced absorption curve. The absorption in the region 10–20 kK is approximately 150 times enlarged relative to the remaining part of the spectrum.

Bottom: Graphic representation of the calculated PPP-CI spectrum of **1**. Full and broken bars represent long axis and short axis polarized transitions, respectively. Thick bars indicate $f > 0.1$, *cf.* Table 2

obtained from the experimental dichroic absorption spectra using the reduction factors [4] $d_{\parallel}^{0} = 0.50$ and $d_{\perp}^{0} = 0.18$. These values were determined from the assumptions that the peaks at 10 kK and 21 kK are purely y- and z-polarized, respectively. The reduction factors obtained for **1** indicate that **1** orients somewhat better than **2** ($d_{\parallel}^{0} = 0.50$, $d_{\perp}^{0} = 0.28$) [5]. **1** probably 'fills its corners' better, although the fact that different brands of polyethylene sheets were used, may account for some of the difference.

The measured spectroscopic data are collected in Table 2 together with the results of a PPP-CI calculation. The transitions predicted by the calculation are indicated schematically in Fig. 5. It appears that the observed positions, polarizations and relative intensities of bands A and B are well reproduced by the calculation.

Above the purely y-polarized 0–0 peak at 9.9 kK, band A shows strongly mixed polarization, with relatively intense z-polarized peaks from 11.7 kK. This is in contrast with the first band of **2**, which is almost purely y-polarized [5]. The z-polarized peaks of **1** appear as a series similar to the y-polarized series of peaks. In both cases the spacing of the peaks is around 1.5 kK. The z-polarized intensity can

Table 2. *Observed and calculated electronic spectrum of azuleno[1,2,3-cd]phenalene* (**1**). Wave numbers are in kK = 1000 cm^{-1}

Observed						PPP-CI Calculation			
Band	ν (0–0)	ν (ε_{max})	ν (vibr.)	log ε^{a}_{max}	Polarization	Symmetry	ν	Predominant Configurations	f
A	9.9	11.4	1.5, 0.3 [b]	2.5	*y*	$^1B_2$	11.2	$7b_1 \leftarrow 4a_2$ (93%)	0.02
B	20.8	20.8	1.4, 0.3	4.7	*z*	$^1A_1$	21.0	$5a_2 \leftarrow 4a_2$ (87%), $7b_1 \leftarrow 6b_1$ (11%)	0.69
C	25.6	25.6	0.3	3.9	*z*				
D	27				*y*	$^1B_2$	29.2	$5a_2 \leftarrow 6b_1$ (43%), $8b_1 \leftarrow 4a_2$ (25%), $9b_1 \leftarrow 4a_2$ (24%)	0.04
E		27.7		4.9	*z*	$^1A_1$	29.9	$7b_1 \leftarrow 6b_1$ (53%), $6a_2 \leftarrow 4a_2$ (30%)	1.59
						$^1B_2$	30.9	$8b_1 \leftarrow 4a_2$ (49%), $5a_2 \leftarrow 6b_1$ (27%)	0.05
						$^1A_1$	31.8	$6a_2 \leftarrow 4a_2$ (34%), $7b_1 \leftarrow 5b_1$ (29%), $7b_1 \leftarrow 6b_1$ (25%)	0.32
		32.1			*y*	$^1B_2$	32.6	$7b_1 \leftarrow 3a_2$ (43%), $8b_1 \leftarrow 4a_2$ (25%), $9b_1 \leftarrow 4a_2$ (14%)	0.02
						$^1A_1$	34.0	$7b_1 \leftarrow 5b_1$ (66%), $6a_2 \leftarrow 4a_2$ (25%)	0.02
						$^1B_2$	34.9	$5a_2 \leftarrow 5b_1$ (79%), $7b_1 \leftarrow 3a_2$ (12%)	0.02
		35.0		4.0	*y*	$^1B_2$	36.6	$9b_1 \leftarrow 4a_2$ (43%), $7b_1 \leftarrow 3a_2$ (19%)	0.28
		38.3		4.2	*z*	$^1A_1$	37.9	$5a_2 \leftarrow 3a_2$ (81%)	0.09
						$^1B_2$	41.5	$6a_2 \leftarrow 6b_1$ (29%), $7b_1 \leftarrow 2a_1$ (19%), $5a_2 \leftarrow 4b_1$ (17%)	0.33
		44.3		4.2	*z*	$^1A_1$	43.5	$7b_1 \leftarrow 4b_1$ (72%), $8b_1 \leftarrow 6b_1$ (12%)	0.02

[a] log ε_{max} values refer to peaks in the cyclohexane solution spectrum [2].
[b] Non-totally symmetric vibration.

hardly be described by a separate electronic transition; the first calculated $\pi^* \leftarrow \pi$ transition of z-polarization is at 21 kK, it has $f = 0.7$ and the observed band B can safely be assigned to it. Introduction of doubly excited configurations in the CI calculations for **2** did not introduce any new states below 30 kK [5], and we find it unlikely that the z-polarized component of band A can be described by a transition to a new electronic state. We find it likely that it is due to vibronic coupling between the first (A) and second (B) electronic states gaining intensity through a non-totally symmetric vibration. Similar cases have been observed *e.g.* for aceheptylene [6] and anthracene [4b]. The vibration seems to have low frequency ($\sim$0.3 kK) and must be of B_2 symmetry.

The shapes of the first bands in **1** and **2** are also quite different. In **2** the 0–0 peak is the strongest in the series, whereas the 0–0 peak in **1** is much weaker than the following y- and z-polarized peaks. According to the *Franck-Condon* principle, this might indicate a significant change in geometry between the ground and first excited state of **1**.

The shape of the band B of **1** is quite similar to the shape of the corresponding band in **2**. The small z-polarized band around 26 kK, C, does not seem to belong to any vibrational fine structure of band B and is not predicted by the PPP-CI calculation using singly excited configurations. Inclusion of doubly excited configurations in the CI procedure may yield a transition in this region, considering the orbital energy picture and the low energy of the first transition (A). The singly excited CI PPP (SCI) calculations on **2** as well as calculations including doubly excited configurations predict a weak y-polarized transition around 28 kK, but no z-polarized transition is predicted between 25 and 30 kK. The MCD. spectra of **2** give some indication of a transition around 27 kK. We feel that band C of **1** probably is due to a fairly weak z-polarized electronic transition with a 0–0 energy of 25.6 kK. The calculations do not predict such a transition, but further studies, experimental (MCD. spectrum) as well as theoretical (large scale CI calculations) may allow a definite assignment. The week y-polarized absorption (band D) around 27 kK can easily be assigned to the calculated transition at 29.2 kK (mainly $5a_2 \leftarrow 6b_1$), but the detailed structure of band D is difficult to determine, because of the overlap with the much more intense band E.

The strong z-polarized E-band is much broader than band B. This can possibly be due to the presence of two strong z-polarized transitions, in agreement with the calculated results, which include strong transitions at 29.9 kK (mainly $7b_1 \leftarrow 6b_1$) and at 31.8 kK (a mixture of several configurations, such as $6a_1 \leftarrow 4a_2$).

Above the region of 30 kK a precise analysis of the bands and their assignment to the numerous calculated electronic transitions is difficult. Under the intense E band the weaker y-polarized absorption starting at 27 kK as discussed above has additional peaks at 32, 35 and 38 kK. The PPP-CI model predicts in this region four y-polarized transitions at 30.9, 32.6, 34.9 and 36.6 kK (see Fig. 5 and Table 2).

In the region between 37 and 45 kK there are two peaks at 38 and 44 kK corresponding to transitions polarized parallel to the z-axis. The calculations predict two z-polarized transitions in this region.

Many of the spectral features can be rationalized from the MO correlation diagram (Fig. 4). The fact that the first band (A) of **1** appears at a considerably lower energy

than the corresponding band in **2** (9.9 *vs.* 13.3 kK) can be understood in simple terms, since both bands are well described by $7b_1 \leftarrow 4a_2$ transitions and the one center transition densities are approximately the same. The simple perturbation method applied to **3** shows that introduction of a bond between atoms 7 and 11 will lower the orbital energy of $7b_1$ approximately by the same amount as introduction of the bond between atoms 6 and 12. The orbital energy of $4a_2$ will be raised the most by introduction of the bond between atoms 6 and 12. It is thus understandable that band *A* in **1** is lower in energy than the corresponding band in **2**. The transition densities of the transitions $7b_1 \leftarrow 4a_2$, and $5a_2 \leftarrow 4a_2$ of **1** are shown below. The

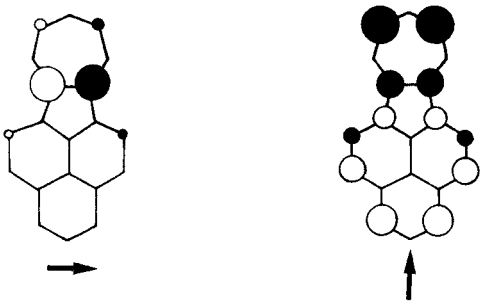

transition densities of **2** are given in [5], where a discussion of the relationship between transition density, singlet-triplet splitting and transition energy is given. For a more complete treatment see [13]. In short, the small transition density of $7b_1 \leftarrow 4a_2$ indicates small splitting between the resulting singlet and triplet, which in turn means that the excitation energy for the singlet will be relatively low.

The second transition (*B*) in **1** and **2** is only quite approximately described by a $5a_2 \leftarrow 4a_2$ transition; considerable contributions come from $7b_1 \leftarrow 6b_1$. The two transitions appear at 20.8 kK (in **1**) and 22.2 kK (in **2**), that is with a much smaller energy difference than for the first transition. This is understandable from Fig. 4, in which the orbital energy difference between $4a_2$ and $5a_2$ is almost the same in the two compounds. Moreover the one center transition density is quite similar in **1** and **2** (see above and [5]).

As for **2** [5] the large energy gap in **1** between bands *A* and *B* can be explained mainly from the fact that the one center transition density is much larger for the second transition, $5a_2 \leftarrow 4a_2$, corresponding to band *B*. This also accounts for the large difference in oscillator strength between the two transitions.

The similarity of the orbitals relevant for the first band of **1** and **2** ($4a_2$ and $7b_1$) with the HOMO and LUMO of azulene [5] [12] makes it possible to predict the shift of the first transition upon methyl substitution in the azulene moiety of **1** and **2**. Assuming the same parameters as for azulene ($\Delta C_1^2 = C_1(7b_1)^2 - C_1(4a_2)^2 = 812$ cm^{-1}) [14], we obtain the following substituent shifts for **1**: positions 6 and 10: 573 cm^{-1}; positions 7 and 9: -141 cm^{-1} and position 8: 743 cm^{-1}. For **2** the result is: positions 6 and 10: 417 cm^{-1}; positions 7 and 9: 550 cm^{-1} and position 8: 275 cm^{-1}.

Experimental part

The synthesis of **1** and **2** has been described in [2] and [3] resp. Freshly purified samples of both compounds were used for the measurements.

The PE. spectra were recorded on a PS 18 instrument of *Perkin Elmer Ltd.* (Beaconsfield, England) equipped with a heated probe. The temperatures to which the samples were heated were 152° for **1** and 134° for **2**. The spectra were calibrated with Ar.

The electronic absorption spectrum of **1** was measured at 77°K on a *Cary 17* spectrometer. A polyethylene sheet was swelled with a chloroform solution of **1**. After evaporation of the solvent and rinsing of the surface with methanol, the sheet was stretched and placed over liquid nitrogen in a quartz dewar.

The dichroic spectra were measured in the manner described by *Eggers et al.* [4]. In the long wavelength region the experiment was performed using 15 polyethylene sheets containing **1** combined to a clear 'thick' sheet through a procedure of heating and pressing. The dichroic absorption curves and baselines were digitalized. The plots of the reduced [4] absorption curves were obtained on a *Hewlett-Packard* 9800–30 computer. The UV./VIS. polarized absorption spectrum of **2** has been reported previously [5].

Calculations. – On **1** and **2** semiempirical calculations were performed using a parametrizised *Hückel*-molecular-orbital (HMO) procedure [8] and the self consistent field method by *Pariser, Parr & Pople* [9] with configuration interaction (PPP-CI). Similar results were obtained by *Zahradník* [15]. For **1** and **2** C_{2v} symmetry was assumed and all bondlengths were set equal to 1.4 Å. The geometry of **1** was taken as three regular hexagons and one regular heptagon. **2** was composed of three regular hexagons and one regular pentagon and the bond angle 6–6a–7 was chosen as 126°.

The CI procedure included 49 singly excited configurations. The electron repulsion integrals in the PPP approximation were calculated according to *Mataga & Nishimoto* [16].

This work was supported by *Fonds der Chemischen Industrie* and *Deutsche Forschungsgemeinschaft*. The stay of *E. W. T.* in Darmstadt was made possible by *DAAD*.

REFERENCES

[1] *E. Heilbronner & H. Bock*, «Das HMO-Modell und seine Anwendung», Vol. 1, Verlag Chemie GmbH, Weinheim 1970; *M. J. S. Dewar & R. Dougherty*, 'The PMO Theory of Organic Chemistry', Plenum Press, New York, London 1975.

[2] *I. Murata, K. Nakasuji, K. Yamamoto, T. Nakazawa, Y. Kayane, A. Kimamma & O. Hara*, Angew. Chem. *87*, 170 (1975); Angew. Chem. Int. Ed. *14*, 170 (1975).

[3] *Ch. Jutz, R. Kirchlechner & H.-J. Seidel*, Chem. Ber. *102*, 2301 (1969).

[4] a) *E. W. Thulstrup, J. Michl & J. H. Eggers*, J. phys. Chemistry *74*, 3868 (1970); b) *J. Michl, E. W. Thulstrup & J. H. Eggers*, Ber. Bunsenges. physik. Chem. *78*, 575 (1974) and references therein.

[5] *E. W. Thulstrup, J. Michl & Ch. Jutz*, Trans. Faraday Soc. *1975*, 1618.

[6] *P. Bischof, R. Gleiter, K. Hafner, M. Kobayashi & J. Spanget-Larsen*, to be published.

[7] *T. Koopmans*, Physica *1*, 104 (1934).

[8] *F. Brogli & E. Heilbronner*, Theoret. chim. Acta (Berl.) *26*, 289 (1972).

[9] *R. Pariser & R. G. Parr*, J. chem. Physics *21*, 466 (1953); *J. A. Pople*, Trans. Faraday Soc. *49*, 1375 (1953).

[10] *P. Bischof & R. Gleiter*, Topics in Nonbenzenoid Aromatic Chemistry; *T. Nozoe et al.*, Edit. Vol. II, Hirokawa Publishing Co., in press.

[11] *P. A. Clark, F. Brogli & E. Heilbronner*, Helv. *55*, 1415 (1972); *J. H. D. Eland & C. J. Danby*, Z. Naturforsch. *23a*, 355 (1968); *M. J. S. Dewar & S. D. Worley*, J. chem. Physics *51*, 263 (1969).

[12] *F. Gerson, J. Jachimowicz & Ch. Jutz*, Helv. *57*, 1408 (1974); *F. Gerson, J. Jachimowicz, I. Murata, K. Nakasuji & K. Yamomoto*, Helv. *58*, 2473 (1975).

[13] *J. Michl & E. W. Thulstrup*, Tetrahedron *32*, 205 (1976).

[14] *E. Heilbronner*, in 'Non Benzenoid Aromatic Compounds', *D. Ginsburg*, Ed., Interscience, New York, N.Y. 1959, p. 171 ff.

[15] *R. Zahradník* in 'Nonbenzenoid Aromatics', *J. P. Snyder*, Edit., Vol. II, Academic Press, New York & London, 1971.

[16] *N. Mataga & K. Nishimoto*, Z. phys. Chem. (Frankfurt) *13*, 140 (1957).